Equivalent Fatigue Damage Growth Parameters for Variable Amplitude Loading

Alexandra Coppe, Matthew J. Pais[1], Nam-Ho Kim[1]

[1]*University of Florida, Gainesville, FL, 32611, USA*
lex.coppe@gmail.com
mpais@ufl.edu
nkim@ufl.edu

ABSTRACT

Fatigue is often assumed to occur under idealized loading conditions where the applied stress is assumed to have constant amplitude. In reality, all service components undergo variable amplitude loading. There are a number of fatigue crack growth models which attempt to predict fatigue under variable amplitude loading, often through the introduction of additional material-specific parameters, which attempt to quantify the interactions between the variable amplitude loading cycles. Uncertainty in the material-specific fatigue parameters can lead to substantially different predictions for crack growth. In this work, synthetic crack size data is generated using a fatigue model suitable for variable amplitude loading. Prognosis is then used to predict the remaining useful life of the component from the crack size data through the identification of component-specific damage growth parameters. A simple fatigue crack growth model is used for prognosis, which does not match the fatigue model used in the generation of the synthetic data. While the identified material properties are different from the true values, they result in comparable life prediction without the need to consider a complex fatigue model during prognosis.[*]

1. INTRODUCTION

There is increasing interest in the use of structural health monitoring (SHM) systems in engineering applications (Sohn, 2004). An SHM system consists of sensors and actuators which are used to actively monitor damage growth (Giurgiutiu, 2008). Based upon this sensor data, decisions about maintenance can be made in a more cost effective manner as maintenance only occurs when it is needed instead of according to some pre-determined schedule.

The conversion of sensor data into estimation of damage location and size is challenging and includes many sources of uncertainty (Li, 2009; Wang, 2005). Once the damage size has been estimated it is necessary to predict the remaining useful life (RUL) of a given component; how long it can continue to be in service until it needs to undergo maintenance. This process is referred to as prognosis.

For aircraft fuselage panels, fatigue crack growth caused by the pressurization cycle associated with each flight is of particular interest. Fatigue crack growth is commonly governed by an ordinary differential equation which considers the effects of the stress intensity factor range ΔK and the stress ratio R (Bedten, 2009) such that

$$\frac{\mathrm{d}a}{\mathrm{d}N} = f\left(\Delta K, R\right). \qquad (1)$$

Fatigue crack growth models are developed by creating functions which agree well with experimental data. As different people will interpret experimental data differently, there are many fatigue crack growth models in the literature (Beden, 2009). The model used to predict fatigue crack growth may be simple or complex depending upon the number of factors which are considered in the model. In general, more complex models require additional experimental data to calibrate an increasing number of material-specific parameters.

It should be noted that there is much uncertainty in the results of fatigue experiments. Consider ten test specimens which are created from a single piece of material. It is likely that each of these ten test specimens will have different fatigue performance and correspondingly predict different values for the

material-specific fatigue model parameters. Through the use of prognosis methods, it is possible to identify component-specific model parameters, and from the predicted model parameters, make an estimate of the remaining useful life (Coppe, 2010a).

It was previously shown that a simple fatigue model can be used in prognosis to account for geometrical effects by identifying equivalent fatigue crack growth model parameters, which although different from the true values, result in accurate remaining useful life estimation (Coppe, 2010b). In this work, this idea is expanded to the case of fatigue crack growth under variable amplitude loading. In reality, all components undergo some variable amplitude loading. During prognosis, a simple fatigue crack growth model is used which does not consider effects such as cycle-specific stress ratio (and correspondingly cycle-specific fatigue model parameters), acceleration or retardation of fatigue crack growth due to load interactions, and the threshold stress intensity factor.

In this paper we will present the crack growth model used in Section 2. Section 3 will introduce the least square filtered method used to identify the damage growth parameters. Results will be introduced in Section 4 and conclusions in Section 5.

2. CRACK GROWTH MODEL

One of the first and simplest fatigue crack growth models is the Paris model (Paris, 1999) which is

$$\frac{\mathrm{d}a}{\mathrm{d}N} = C\left(\Delta K\right)^m \tag{2}$$

where da/dN is the crack growth rate, m is the slope of the linear portion of the da/dN-ΔK curve and C is the y-intercept of the linear portion of the da/dN curve at ΔK = 1. The values C, m, and ΔK_{th} are shown in Figure 1.

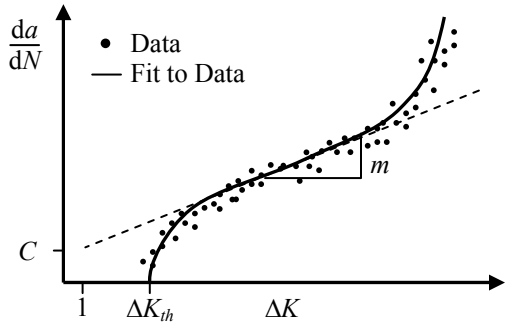

Figure 1. Crack growth data and Paris model fit.

The Paris model does not consider the threshold stress intensity factor ΔK_{th}, below which no crack growth will occur. For different stress ratios R unique values of C and m must be identified (Sun, 2006) as shown in Figure 2. The classical Paris model does not consider the load interactions created by crack tip plasticity due to variable amplitude loading and therefore is not suitable for predicting fatigue crack growth due to variable amplitude loading.

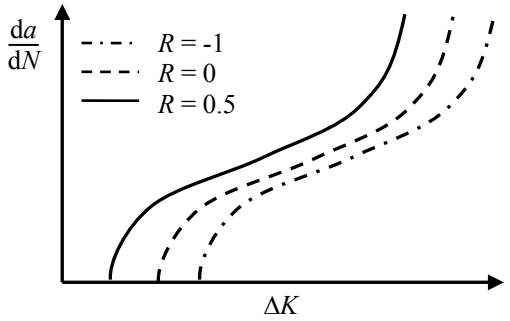

Figure 2. Fatigue crack growth curves for different stress ratios R for constant amplitude loading.

For a center crack in an infinite plate subjected to Mode I loading, the stress intensity factor range ΔK is given as (Tada, 1987)

$$\Delta K = \Delta\sigma\sqrt{\pi a} \tag{3}$$

where $\Delta\sigma$ is the applied stress range and a is the half crack length. The half crack length a_i at the i^{th} cycle derived from combining Eq. (3) into Eq. (2) and integrating from the initial crack size a_o to a_i is given as

$$a_i = \left[N_i C\left(1-\frac{m}{2}\right)\left(\Delta\sigma\sqrt{\pi}\right)^m + a_o^{1-\frac{m}{2}} \right]^{\frac{2}{2-m}} \tag{4}$$

where N_i is the number of applied loading cycles since $a_i = a_o$. Similarly, the number of cycles to failure N_f for a center crack in an infinite plate can be derived by rearranging Eq. (4) as

$$N_f = \frac{a_c^{1-\frac{m}{2}} - a_o^{1-\frac{m}{2}}}{C\left(1-\frac{m}{2}\right)\left(\sigma\sqrt{\pi}\right)} \tag{5}$$

where a_c is the critical crack size. Note that N_f is uncertain because the initial crack size and damage growth parameters are uncertain. Since the critical crack size is generally unknown, a threshold crack size can be selected. Once the current crack size exceeds the threshold, maintenance should be performed.

Xiaoping (2008) introduced a modified version of the Paris model which addresses some of the inconveniences and limitations associated with the classical Paris model for fatigue crack growth under variable amplitude loading. In modified Paris model, the crack growth rate follows the following relationship

$$\frac{\mathrm{d}a}{\mathrm{d}N} = C\left[\left(M_R M_P \Delta K\right)^m - \Delta K_{th}^m\right]. \tag{6}$$

In Eq. (6) M_R adjusts the crack growth rate according to nonzero stress ratios, which allows for a single value of C and m to be used for any R-ratio as shown in Figure 3. Note that the independent fatigue curves from Figure 2 have been condensed to nearly a single curve though the use of M_R in Figure 3. This is particularly convenient in the variable amplitude framework where each cycle may have a distinct R-ratio, which would require cycle-dependent C and m in the classical Paris model. The parameter M_R requires the introduction of two material constants β and β_1 for the conversion of $R \neq 0$ to $R \approx 0$ and is given as

$$M_R = \begin{cases} (1-R)^{\beta_1} & -5 \le R < 0 \\ (1-R)^{\beta} & 0 \le R < 0.5 \\ \left(1.05 - 1.4R + 0.6R^2\right)^{\beta} & 0.5 \le R < 1 \end{cases} . \quad (7)$$

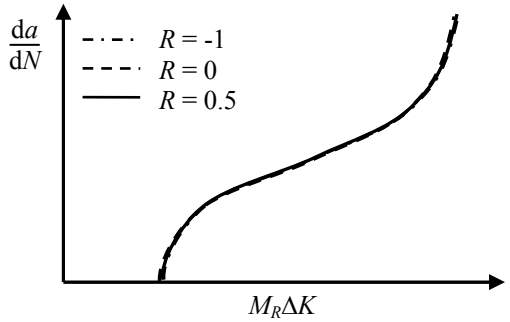

Figure 3. Effect of the modified Paris parameter M_R.

The parameter M_P in Eq. (6) modifies the crack growth rate due to the interactions in the plastic zones for variable amplitude loading through the introduction of the material constant of the exponent n, which is identified from some overload and underload conditions and is given as

$$M_P = \begin{cases} \left(\dfrac{r_y}{a_{OL} + r_{OL} - a_i - r_\Delta} \right)^n & a_P < a_{P,OL} \\ 1 & a_P \ge a_{P,OL} \end{cases} \quad (8)$$

where a_p is the sum of the crack and plastic zone size

$$a_P = a_i + r_y \quad (9)$$

and a_{OL} is the largest previous crack tip and plastic zone size given as

$$a_{P,OL} = a_{OL} + r_{OL} - r_\Delta . \quad (10)$$

The plastic zone radius for the current crack geometry is given by

$$r_y = \alpha \left(\frac{K_I^{\max}}{\sigma_y} \right)^2 \quad (11)$$

where α is a geometric plastic zone correction factor, $K_I^{\max}$ is the Mode I stress intensity factor at the maxima for the current cycle, and σ_y is the yield stress for the specified material. The plastic zone radius when the largest overload occurred is given as

$$r_{OL} = \alpha \left(\frac{K_I^{OL}}{\sigma_y} \right)^2 \quad (12)$$

where K_I^{OL} is the Mode I stress intensity factor when the overload occurred. Finally, the reduction in the plastic zone size due to an underload r_Δ follows

$$r_\Delta = \alpha \left(\frac{K_{I,i-1}^{\min} - K_{I,i}^{\min}}{\sigma_y} \right)^2 \quad (13)$$

where $K_{I,i-1}^{\min}$ and $K_{I,i-1}^{\min}$ are the Mode I stress intensity factors at the minima of the previous and current loading cycles. The plastic zone correction factor α was determined from elastic-plastic finite element analysis (Xiaoping, 2008) for a range of geometric factors and is given as

$$\alpha = 0.35 - \frac{0.29}{1 + \left[1.08 \left(K_I^{\max} \right)^2 / \left(t\sigma_y^2 \right) \right]^{2.15}} \quad (14)$$

where t is the thickness of a given panel. Additional plastic zone correction factors are available for plane stress or plane strain conditions (Xiaoping, 2008). The various crack and plastic zone sizes detailed in Eqs. (8) - (13) are shown in Figure 4. Note that the plastic zone diameters are shown in Figure 4, while the radii are specified in Eqs. (8) - (13).

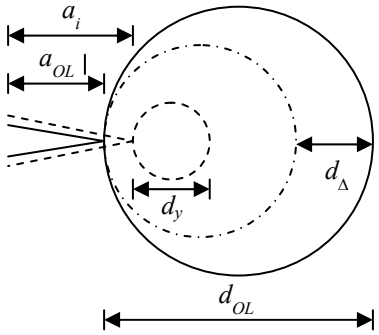

Figure 4. The current, overload, and underload crack geometries and plastic zones used in M_P.

In order to reduce the uncertainty in damage growth we identify the damage growth parameters. The next section introduces the identification method we chose, least square filtered Bayesian (LSFB).

3. LEAST SQUARE FILTERED BAYESIAN (LSFB) METHOD

The LSFB method (Coppe, 2010a) processes information collected at every cycle by least square fit in order to reduce the noise, and identify the bias, *b*. The least square problem is expressed as

$$\min_{a_o,m',b} \sum_i \left(a_i^{meas} - b - a_i \right)^2 \qquad (15)$$

where a_i^{meas} are the measured crack sizes, in this case due to the absence of actual data we use synthetic one with noise model to simulate measurement data. The synthetic measured crack sizes used in Eq. (15) are predicted according to the modified Paris model. Let a_i^{true} be the damage size generated using the modified Paris model, the synthetic data can be defined as

$$a_i^{meas} = a_i^{true} + v \qquad (16)$$

where v is the noise uniformly distributed with an amplitude of 2 mm.

The LSFB method assumes that the fatigue crack growth under variable amplitude loading can be predicted using the classical Paris model from Eq. (2) through the identification of equivalent damage growth parameters *C*' and *m*', which although different from the true C and *m* used in the generation of the synthetic data, results in equivalent prediction in the crack growth rate for the classical and modified Paris models as

$$\frac{da}{dN} = C'(\Delta K)^{m'} = C\left[\left(M_R M_P \Delta K \right)^m - \Delta K_{th}^m \right] \qquad (17)$$

and accordingly, the same remaining useful life. Note that here a value is assumed for *C*' and only *m*' is identified. Different metrics (e.g. maximum, mean, and median) for the stress range $\Delta\sigma$ in Eq. (3) are chosen to represent the variable amplitude load history and are tested for each example problem. The identified values of a_o, *m*' and *b* are then used to generate a new estimate of the damage size at the i^{th} cycle using Eq. (4), this estimate is denoted filtered data. The filtered data are then used in Bayesian updating in order to narrow down the distribution of *m*' and obtain a more accurate prognosis. The identified a_0 and *b* are considered as deterministic, and only uncertainty in *m*' is considered in the Bayesian update.

Bayesian inference is based on the Bayes' theorem on conditional probability. It is used to obtain the updated (also called posterior) probability of a random variable by using new information. In this paper, since the probability distribution of *m*' given *a* is of interest, the form of Bayes' theorem is used as (An, 2008)

$$f_{updt}(m') = \frac{l(a \mid m') f_{ini}(m')}{\int_{-\infty}^{+\infty} l(a \mid m') f_{ini}(m') dm'} \qquad (18)$$

where f_{ini} the assumed (or prior) probability density function (PDF) of *m*', f_{updt} the updated (or posterior) PDF of *m*' and $l(a|m)$ is called the likelihood function, which is the probability of obtaining the characteristic crack length *a* for a given value of *m*', the derivation of the likelihood function can be found in previous work (Coppe, 2010b).

The likelihood function is designed to integrate the information obtained from SHM measurement to the knowledge about the distribution of *m*'. Instead of assuming an analytical form of the likelihood function, uncertainty in measured crack sizes is propagated and estimated using Monte Carlo simulation (MCS). Although this process is computationally expensive, it will provide accurate information for the posterior distribution.

Once the distribution of *m*' has been identified at cycle N_i, it can be used to predict the RUL. The distribution of RUL is calculated at every SHM measurement cycle N_i using MCS and the RUL is estimated using Eq. (5) derived from Paris' law. This allows us to estimate the distribution and from there obtain the 5th percentile.

The 5th percentile of N_f samples is used as a conservative estimate of RUL in order to have a safe prediction. Since random noise is added to the synthetic data, the result may vary with different sets of data. Thus, the above process is repeated with 100 sets of measurement data and mean plus and minus one standard deviation intervals are plotted.

In order to show the value of the LSFB method the RUL calculated using the distribution of *m*' and the distribution (mean ± one standard deviation) of the 5th percentile of the distribution of RUL obtained using the updated distribution of *m*' at each inspection are compared to the true RUL.

4. RESULTS

For each example, a center crack of initial length 10 mm in an infinite plate of aluminum 7075-T6 square plate was used. Crack growth was predicted under the block loading spectrum shown in Figure 5 until the crack reached a size of 50 mm. In this approach, these 50 loading cycles shown in Figure 5 are repeated until the critical crack size is reached. Random loading which does not follow the block loading diagram was also considered where crack growth was modeled until the same critical crack size was reached.

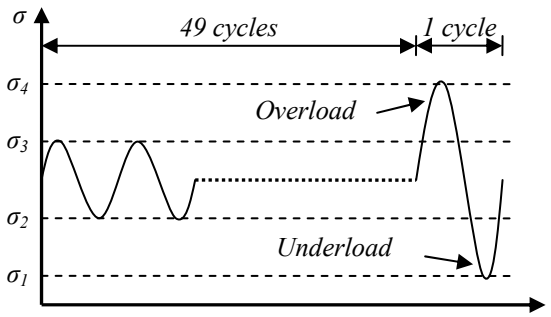

Figure 5. Repeating block loading used for simple variable amplitude fatigue predictions.

The values used in the modified Paris model for the generation of variable amplitude fatigue crack growth data are given in Table 1.

Table 1. Variables data used to generate the synthetic data

Variable	Value
M	3.21
C	6.85E-11
β	0.70
β_1	0.84
N	0.30
ΔK_{th} (MPa $\sqrt{\text{m}}$)	2.2
σ_y (MPa)	520

The relatively large initial crack size (10mm) is chosen because many SHM sensors cannot detect small cracks. In addition, there is no significant crack growth when the size is small. This initial crack size is still too small to be a risk for an airplane.

True crack growth data was calculated using the modified Paris model. A noise model was then applied to the true crack growth data to approximate the effect of noise in sensor data. The characteristic crack length at each iteration was then used in the identification of an equivalent Paris model exponent m' through the use of the least-square-filtered Bayesian method. The value of C' is fixed at 7.00E-11 and m' initially follows a uniform distribution between 2 and 5. Due to the non-constant stress amplitude, three cases for the stress range are considered: the maximum, mean, and median stress range up to the current inspection.

Example problems which are presented include: block loading with an overload every 50 cycles, block loading with an underload every 50 cycles, and randomly generated loading. Under this block loading, the stresses shown in Figure 5 are σ_1 = 150 MPa, σ_2 = 150 MPa, σ_3 = 250 MPa, and σ_4 = 350 MPa. All crack growths are calculated using the modified Paris model integrated using the forward Euler method for ΔN = 1. A comparison of the crack size as a function of cycle number for the various approaches and stress values is given in Figure 6 where the constant amplitude curve is for 150 to 250 MPa.

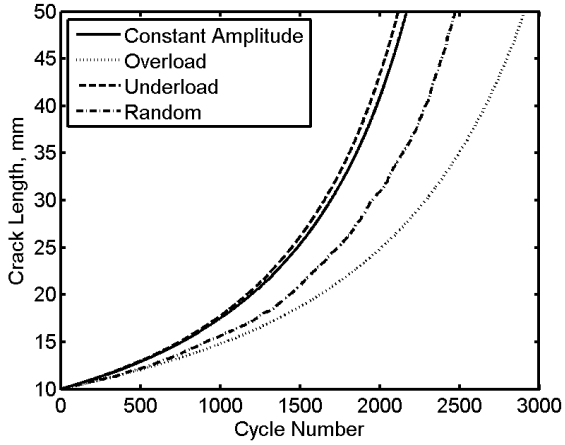

Figure 6. Effect of overload and underload on crack length at a given cycle number.

Compared to the case of constant amplitude loading, the presence of an underload in the block loading reduces the crack tip plasticity. The reduction in the crack tip plasticity results in increased crack growth compared the constant amplitude loading case. While the chosen loading does not represent a largely different crack growth rate for underload or constant amplitude loading, this is load history dependent and in some cases should be considered. The overloads, accelerate crack growth during the overload cycle and then slow subsequent crack growth. For the chosen block loading, the retardation due to the overload has a stronger effect than the crack growth acceleration during the overload cycle, resulting in an overall decrease in the crack growth rate. The combined effects of an overloads and underloads during the random loading case combines create crack growth which is slower than the constant amplitude, but faster than the case of only overloads.

4.1 Block loading with an overload

The first test case for variable amplitude loading is that of block loading with an overload. The overload every 50 cycles increases the plasticity at the crack tip, which retards crack growth under the following constant amplitude loading cycles. The effect of the non-constant crack tip plasticity explains why the crack growth curve in Figure 6 for the overload case has the longest life.

The distribution of the 5th percentile of the estimate RUL distribution is given in Figure 7 with three different $\Delta\sigma$: maximum, mean, and median. In Figure 7 the mean and median RUL are largely identical. It can be noticed that the RUL estimate for all three stress ranges converge to the theoretical value, however it can be noted that the mean and median values of stress

represent conservative estimates, while the maximum stress is unconservative. It should also be noted that there is less uncertainty for the case of maximum stress range

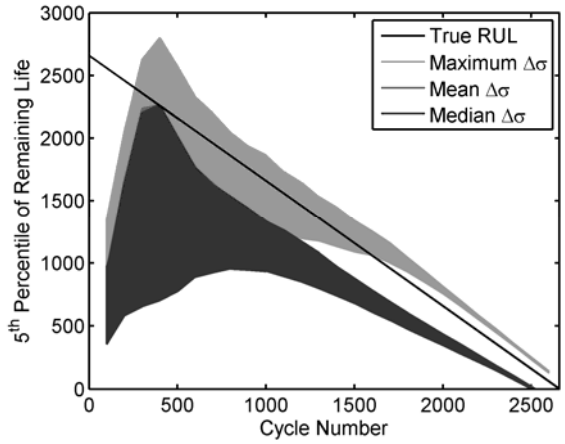

Figure 7. Distribution of the 5th percentile of RUL estimation for block loading with an overload for three stress ranges.

In Figure 8 the evolution of the error in the maximum likelihood of the RUL is given. It should be noted that as more measurement data is included in the prognosis, the error reduces and the uncertainty in the error also decreases. As with the RUL figure, it can be noted that the mean and median stress ranges represent conservative (e.g. positive errors) while the maximum stress range represents an unconservative estimation of the RUL.

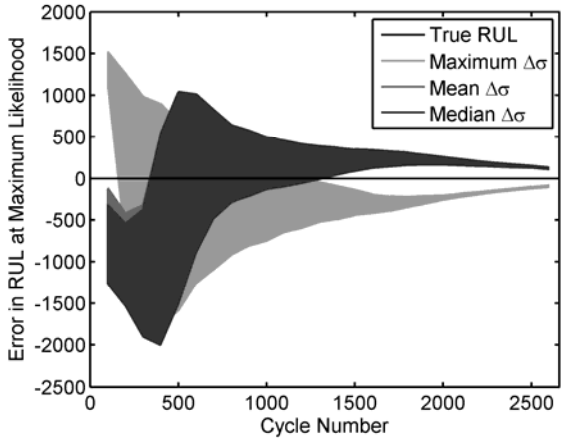

Figure 8. Distribution of the 5th percentile of error in RUL for overload block loading at maximum likelihood for three stress ranges.

4.2 Block loading with an underload

The first test case for variable amplitude loading is that of block loading with an underload. Under this block loading, the stresses shown in Figure 5 are σ_1 = 50 MPa, σ_2 = 150 MPa, σ_3 = 250 MPa, and σ_4 = 250 MPa. The underload every 50 cycles decreases the plasticity at the crack tip, which accelerates crack growth under the following constant amplitude loading cycles. The effect of the non-constant crack tip plasticity explains why the crack growth curve in Figure 6 for the underload has the shortest life.

The LSFB analysis for the RUL is given in Figure 9. For the case of block loading with an underload, it can be noticed from Figure 9 that again the mean and median stress ranges largely overlap one another. For this stress history, the maximum stress range again is offset above the mean and median stress ranges, but this time it converges to a more accurate RUL estimation. While this solution is more accurate, it converges from the unconservative side.

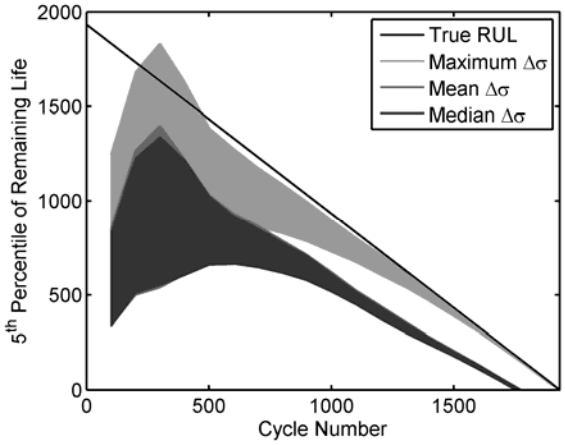

Figure 9. Distribution of the 5th percentile of RUL estimation for block loading with an underload for three stress ranges.

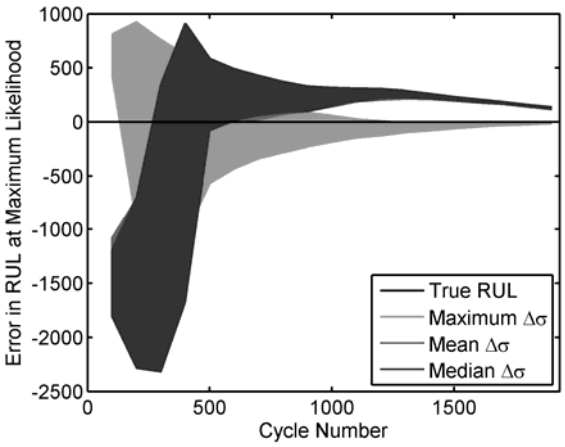

Figure 10. Distribution of the 5th percentile of error in RUL for underload block loading at maximum likelihood for three stress ranges.

In Figure 10 the evolution of the error in the RUL at the maximum likelihood estimate is given. As before, as more inspection data is given to the LSFB prognosis method, the more the bounds on the RUL estimate

reduce independent of the choice of stress range. While the maximum stress range seems to show a more accurate answer this solution does have a negative (e.g. unconservative) error, while the mean and median stress ranges have a positive (e.g. conservative) error.

4.3 Random fatigue loading

For this case, random stress data in MPa was generated where for a particular cycle the maximum and minimum stress follow the relationship

$$\begin{aligned} \sigma_{\max} &= 100r_1 + 100r_2 + 100 \\ \sigma_{\min} &= 50r_3 + 50r_4 \end{aligned} \tag{19}$$

where r_1, r_2, r_3, and r_4 are randomly generated values between 0 and 1 and the resulting maximum and minimum stress profiles are given in Figure 11. It was chosen to use two random numbers at each loading cycle in the generation of the random stress history in order to increase the effect of the M_P corrector in the modified Paris model used in the generation of the data. This represents acceleration and retardation of the crack growth rate in the data which is completely missed in the Paris model which is used in the prognosis model. The maximum and minimum stress curves for this case are shown in Figure 11.

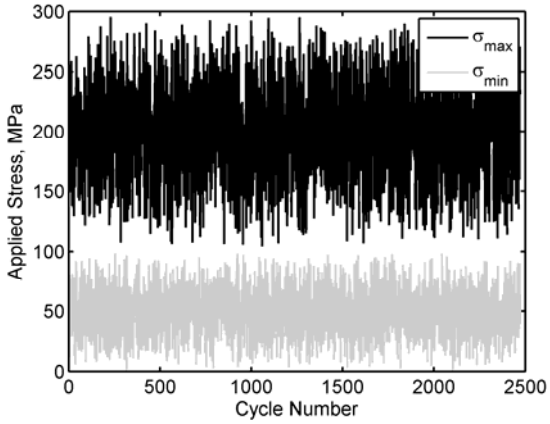

Figure 11. Randomly generated stress history.

The LSFB analysis for the RUL is given in Figure 12. For the case of a randomly generated stress range, the mean and median stress ranges show the best agreement with the true RUL, and while they are unconservative at one point, at the point of failure the RUL estimate is conservative. There is error for the maximum stress range case which is similar to that in the previous stress histories.

The error in the RUL estimate at the maximum likelihood is given in Figure 13. Again it can be seen that the maximum stress range converges from the unconservative side. The mean and median errors in RUL are largely identical again, except for some small differences prior to cycle number 1000.

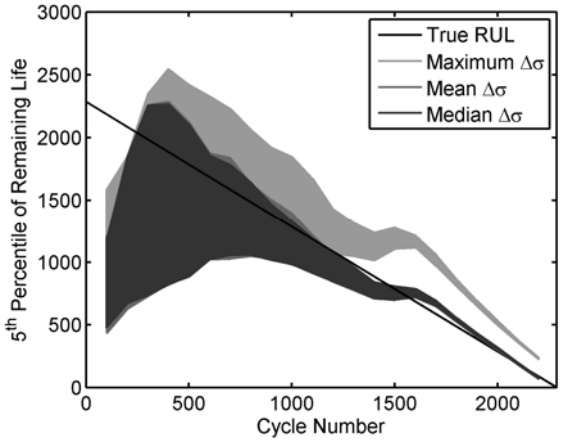

Figure 12. Distribution of the 5th percentile of RUL estimation for random stress history for three stress ranges.

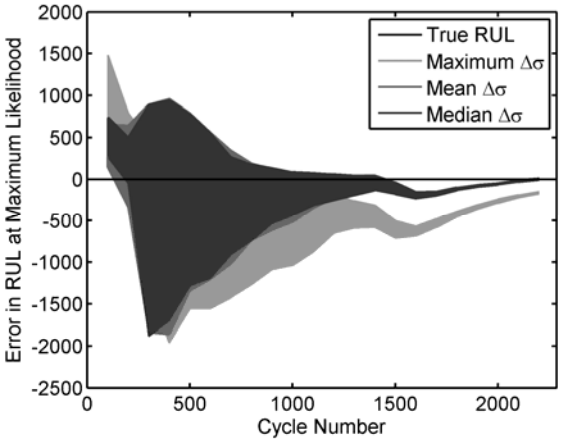

Figure 13. Distribution of the 5th percentile of error in RUL for random loading at maximum likelihood for three stress ranges.

It should be noted that in this case, the true behavior represents significant difference from the assumptions of the classical Paris model. Each cycle will have a unique stress ratio R. In the classical Paris model this would manifest as different values of C and m for every cycle. Furthermore, the interaction between loads obscures the true crack growth behavior by accelerating and retarding the crack growth rate. To largely capture this behavior through identification of a single parameter m' is significant, especially with the level of simplification that is possible in the underlying model as a result of choosing a simple fatigue crack growth model for use in prognosis.

5. CONCLUDING REMARKS

In this work, the application of the least-squares filtered Bayesian method to variable amplitude loading was considered. Due to the complexity and number of fatigue model parameters commonly associated with modeling variable amplitude fatigue a simple fatigue model, the classical Paris model, was used in the prognosis of simulated variable amplitude crack size data. This model neglects to consider many of the effects which are crucial when modeling variable amplitude loading including: the dependence of C and m on the stress ratio R, crack growth rate acceleration following an underload, and crack growth rate retardation following an overload. However, the LSFB method identifies an single equivalent value for the fatigue model parameter m which results in accurate estimations of the RUL without the need to consider a complex fatigue model within the prognosis algorithm.

Three cases were considered for defining the stress range used in the classical Paris model as part of the LSFB prognosis: the maximum stress up to the current inspection, the mean stress up to the current inspection, and the median stress up to the current inspection. While results were satisfactory regardless of the choice of stress range, the mean and median stress ranges tended to have conservative RUL estimates while the maximum stress range was typically unconservative.

In the future, this would could be extended to consider the case of geometrical effects along with variable amplitude fatigue loading. The authors have shown independently that equivalent values of the Paris model exponent m can be identified for geometrical effects or variable amplitude fatigue loading. The combination of both of these conditions would represent a significant difference between reality and the simple prognosis model and further diversity this prognosis method for a range of cracked geometries and loading conditions.

ACKNOWLEDGMENT

This work was supported by the Air Force Office of Scientific Research under Grant FA9550-07-1-0018 and by the NASA under Grant NNX08AC334.

NOMENCLATURE

a	characteristic crack size
a_c	critical crack size
a_i	characteristic crack size at cycle N_i
a_i^{meas}	synthetic measured crack size at cycle N_i
a_{OL}	crack size when overload occured
b	deterministic bias
C	Paris model constant
C'	equivalent Paris model constant
$K_I^{\max}$	maximum Mode I stress intensity factor
K_I^{OL}	Mode I stress intensity factor at overload
$K_{I,i-1}^{\min}$	minimum Mode I stress intensity at cycle i-1
$K_{I,i}^{\min}$	minimum Mode I stress intensity at cycle i
M_R	modified Paris model corrector for R
M_P	modified Paris model corrector for plasticity
m	Paris model exponent
m'	equivalent Paris model exponent
N_f	number of cycles to failure
n	M_P acceleration/retardation exponent
R	ratio of minimum to maximum stress
r_y	plastic zone radius for current crack
r_{OL}	plastic zone radius for a_{OL}
r_Δ	reduction in plastic zone due to underload
t	plate thickness
α	plastic zone correction factor
β	M_R exponent for positive R
β_1	M_R exponent for negative R
ΔK	stress intensity factor range
ΔK_{th}	threshold stress intensity factor range
$\Delta\sigma$	stress range
σ_{max}	maximum stress for a given cycle
σ_{min}	minimum stress for a given cycle
σ_y	yield stress

REFERENCES

An, J., Acar, E., Haftka, R. T., Kim, N. H., Ifju, P. G., Johnson, T. F. (2008) Being conservative with a limited number of test results, *Journal of Aircraft*, vol. 45, pp. 1969-1975.

Beden, S., Abdullah, S., Ariffin, A. (2009). Review of fatigue crack propagation models in metallic components, *European Journal of Scientific Research*, vol. 28, pp. 364-397.

Coppe, A., Haftka, R. T., Kim, N. H. (2010a). Least squares-filtered Bayesian updating for remaining useful life estimation, in *Proceeding of AIAA Non-Deterministic Approaches Conference*, Orlando, FL.

Coppe, A., Pais, M., Kim, N. H., Haftka, R. T. (2010b) Identification of equivalent damage growth parameters for general crack geometry, in *Proceeding of Annual Conference of the Prognostics and Health Management Society 2010*, Portland, OR.

Giurgiutiu, V. (2008) Structural Health Monitoring with Piezoelectric Wafer Active Sensors, *Academic Press*, Burlington, MA.

Li, G., Yuan, F. G., Haftka, R. T., Kim, N. H. (2009). Bayesian segmentation for damage images using MRF prior, *Sensors and Smart Structures Technologies for Civil, Mechanical and Aerospace Systems*, vol. 7292, pp. 72920J-12.

Paris, P. C., Tada, H., Donald, J. K. (1999) Service load fatigue damage – A historical perspective,

International Journal of Fatigue, vol. 21, pp. 35-46.

Tada H., Paris, P., Irwin, G. (1987) Stress Analysis of Cracks Handbook, *ASME Press*, New York, NY.

Sohn, H., Farrar, C., Hemez, F., Czarnecki, J., Shunk, D., Stinesmates, D., Nadles, B. (2004) A Review of Structural Health Monitoring Literature: 1996-2001, *Report Number LA-12976-MS*, Los Alamos National Laboratory, Los Alamos, NM.

Sun, C. T. (2006) Mechanics of Aircraft Structures, *John Wiley and Sons*, Hoboken, NJ.

Wang, L., Yuan, F. G. (2005). Damage identification in a composite plate using prestack reverse-time migration technique, *Structural Health Monitoring*, vol. 4, pp. 195-211.

Xiaoping, H., Moan, T., Weicheng, C. (2008) An engineering model of fatigue crack growth under variable amplitude loading, *International Journal of Fatigue*, vol. 30, pp. 2-10.

Alexandra Coppe is an Assistant Research Scientist at CALCE at the University of Maryland. She received her B.S. and M.S. degrees in Applied Mathematics from the University Paul Sabatier, Toulouse, France in 2005 and 2007. She received her M.S. and Ph.D. degrees in Mechanical Engineering in 2010 from the University of Florida. Her research interests are structural health management, fracture mechanics, non-deterministic methods and model parameter identification methods such as Bayesian inference.

Matthew Pais received his B.S. degree in Mechanical Engineering from the University of Missouri in 2007. He received his M.S. degree in Mechanical Engineering from the University of Florida in 2009 and is currently pursuing his Ph.D. in Mechanical Engineering at the University of Florida. His research interests are computational fracture mechanics, finite element methods, optimization, and surrogate modeling.

Nam-Ho Kim is an Associate Professor of Mechanical and Aerospace Engineering at the University of Florida. He graduated with a Ph.D. in the Department of Mechanical Engineering from the University of Iowa in 1999. His research area is structural design optimization, design sensitivity analysis, design under uncertainty, structural health monitoring, nonlinear structural mechanics, and structural-acoustics. He has published more than hundred refereed journal and conference papers in the above areas.